

# A study on stability analyses of reinforced embankments based on centrifugal model tests

E. Taniguchi & Y. Koga

Public Works Research Institute, Tsukuba, Japan

S. Yasuda

Kyushu Institute of Technology, Kitakyushu, Japan

I. Morimoto

Kiso-jiban Consultants Co., Ltd, Tokyo, Japan

**ABSTRACT:** Centrifugal model tests were performed for embankments reinforced with non-woven fabric by tilting the models and applying vertical load to them. The test results showed that the fabric reinforcement can sufficiently strengthen embankments to prevent their collapse. Stability analyses assuming a circular slip surface showed good agreement with the centrifugal model tests.

## 1 INTRODUCTION

Centrifugal model tests were performed on embankments reinforced by non-woven fabric. The purposes of model tests were 1) to grasp the effects of the length of fabric reinforcement on the stability of embankments against surcharge and horizontal force, and 2) to comprehend the validity of a simplified stability analysis which takes into account fabric reinforcement.

## 2 CENTRIFUGAL TESTING APPARATUS

A Centrifugal testing apparatus of the Public Works Research Institute, was used in the tests. The effective radius of the apparatus is 1.15m, and maximum centrifugal acceleration is 300G.

## 3 MATERIAL AND SCALING LAW

A model ground and embankment was constructed using Toyoura sand dried in the air. Static triaxial tests (CD) on Toyoura sand of the same density as that in the model showed that cohesion  $C$  was 0 and the angle of internal friction  $\phi$  was 43.4 degrees.

Table 1 shows the physical properties of the non-woven fabric used in the tests. These data were obtained from uniaxial tension tests using a cylindrical fabric (diameter = 50mm).

The following scaling law was adopted in this series of tests; the reinforcement ratio  $R$  (non-dimension, Tatsuoka et al. (1985)) defined by the following equation coincides in the model and the prototype. Poisson's ratio  $\nu$  of the non-woven

fabric is assumed to be zero.

$$R = \frac{(-\bar{\epsilon}_{3R}) E \cdot t}{\sigma_{30} \cdot \Delta H} \quad (1)$$

where  $\bar{\epsilon}_{3R}$ : average tensile strain of reinforced soil in the horizontal direction ( $\bar{\epsilon}_{3R} < 0$ ),  $E$ : Young's modulus of reinforcing material,  $t$ : thickness of reinforcing material,  $\sigma_{30}$ : horizontal confining pressure acting on reinforced soil,  $\Delta H$ : spacing of reinforcing material.

A centrifugal model test provides the condition,  $(\bar{\epsilon}_{3R})_m / (\bar{\epsilon}_{3R})_p = 1$  and  $(\sigma_{30})_m / (\sigma_{30})_p = 1$  ( $m$ : model,  $p$ : prototype). Therefore in order to take  $(R)_m$  equal to  $(R)_p$ , the following equation should hold.

$$\frac{(E)_m(t)_m}{(E)_p(t)_p} = \frac{(\Delta H)_m}{(\Delta H)_p} = \frac{1}{n} \quad (2)$$

where  $\frac{1}{n}$ : model scale

If the height of the actual embankment is assumed to be 5 m, the  $1/n$  becomes  $1/50$ . And if two kinds of prototype non-woven fabric, whose young's modulus and thickness are shown in Table 2, are selected in the tests, the value of  $(E)_m(t)_m / (E)_p(t)_p$  is  $1/50.4$  and  $1/55.1$ , respectively. Therefore the use of this non-woven fabric essentially satisfies the scaling law described above. Actually 50G centrifugal acceleration is applied to the  $1/50$  scaled model.

## 4 TEST PROCEDURES

Eleven tests were performed using the models shown in Fig. 1. Table 3 shows the test conditions. Centrifugal accelerations

of 50G and 100G were applied to the models. Air dried Toyoura sand was air pluviated to the container and model ground, and an embankment with the relative density of about 90% was constructed.

The embankments have an inclined slope and a vertical slope in series I and II, respectively. In latter case, the vertical slope was protected by four sandbags, 2.5cm in diameter. These non-woven fabric sandbags contained Toyoura sand. The sandbag and reinforcing fabric were sewn together.

To reduce the friction between the soil model and the side walls of the container,

grease (Dow Corning, for high vacuum) was applied to the side walls to a thickness of 100  $\mu$ m. One side wall consisted of glass, and the other, of steel. A latex membrane, 0.2mm thick, was placed between the side wall and the soil model. As a mesh was drawn on the membrane at 5mm intervals, the deformation of the soil model could be measured from the deformation of the mesh.

To apply horizontal seismic force to the models, the models were tilted up to 16 degrees for Tests No. 6 to No. 8, and photographs were taken at the tilting angles of 2, 4, 6, 8, 10, 12 and 16 degrees. In the other tests a steel plate, 50mm in length and 100mm in width, 15mm in height, 210gf in weight, was placed on the top of the embankment, and a static load was vertically applied to the plate by a hydraulic piston. Strain controlled loading was adopted, and the loading speed was 0.012 mm/sec. The applied load and the settlement of embankment were measured using a load cell and displacement gauge which were installed on the piston.

Table 1 Properties of non-woven fabric

material	nylon 70%, polyester 30%
thickness (mm)	0.217
tensile strength at peak $\sigma_t$ (kgf/cm <sup>2</sup> )	13.2 - 13.6
strain at peak $\epsilon_t$ (%)	38 - 29
young's modulus at $\epsilon = 15\%$ $E_{15}$ (kgf/cm <sup>2</sup> )	47.3 - 57.3

Table 2 Data for non-woven fabric of model and prototype

model		prototype		$\frac{(E \cdot t)_m}{(E \cdot t)_p}$
Young's modulus E (kgf/cm <sup>2</sup> )	thickness t (mm)	Young's modulus E (kgf/cm <sup>2</sup> )	thickness t (mm)	
56.3	0.217	200	3.08	1
		150	4.49	55.1

Table 3 Test conditions

series No	test No	model No	centrifugal acceleration (G)	relative density of model ground and embankment (%)	reinforcement length and number of fabrics	method of loading
I	1	I-A	100	89.8	0 sheet	applying vertical loads
	2	I-B		90.0	307mm X 4 sheet	
	3	I-B		87.2		
	4	I-A	50	91.7	0 sheet	
	5	I-C		84.3	307mm X 6 sheet	
II	6	II-A	50.1	87.3	60mm X 4 sheet	tilting models
	7	II-B	50.8	87.3	100mm X 4 sheet	
	8	II-C	49.7	87.1	150mm X 4 sheet	
	9	II-D	50.2	90.7	60mm X 4 sheet	applying vertical loads
	10	II-E	49.6	87.4	100mm X 4 sheet	
	11	II-F	52.4	87.4	242mm X 4 sheet	

Reinforcement lengths of fabrics in series I show average value among all sheets.

## 5 TEST RESULTS

Fig. 2 shows the relationship between the applied load and the settlement of the embankment with an inclined slope. Tests No. 2 and No. 5 were stopped before the load reached a peak value, because of the limitation of the capacity of the piston. Fig. 2 (b) indicates that the peak value of the load in the reinforced embankment (Test No. 3) was 19% larger than that in the un-reinforced one (Test No. 4), and the settlement when the load was at the peak. In the region where the settlement was larger than 4mm (=4% of the height of

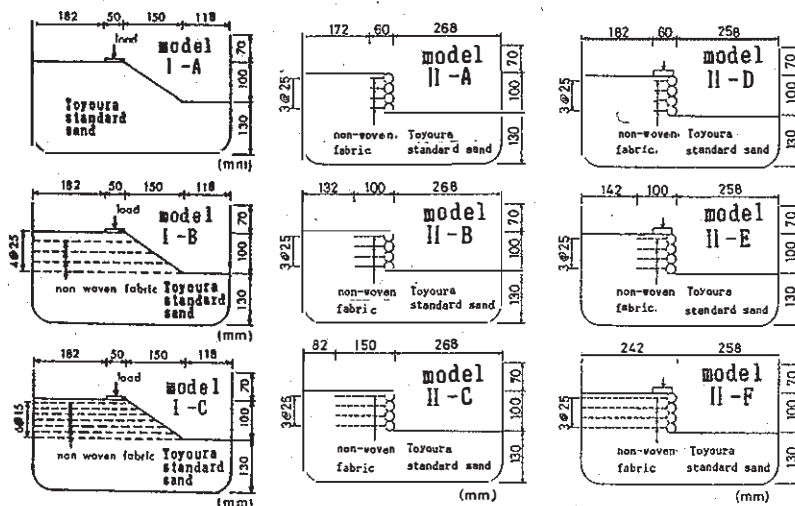


Fig. 1 Models used in tests

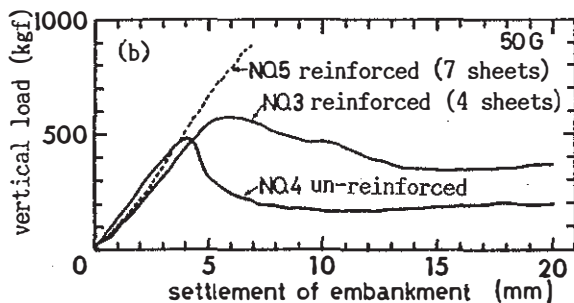
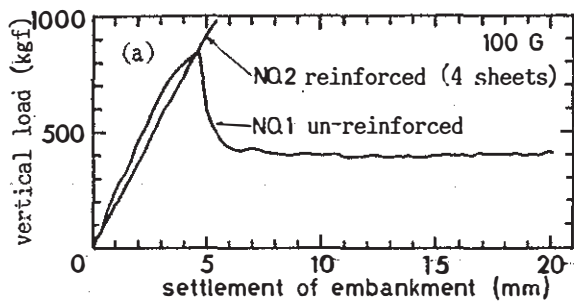


Fig. 2 Vertical load and settlement of top of embankment

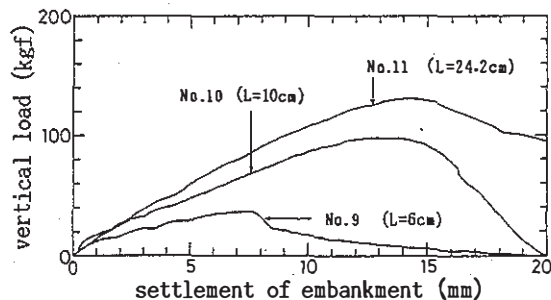


Fig. 3 Vertical load and settlement of top of embankment

embankment), the load in the reinforced embankment was larger than that in the un-reinforced one for the same settlement, and this was caused by the fabric reinforcement. However in the region where the settlement was less than 4mm, the load in the reinforced embankment was slightly less than that in the un-reinforced one. Therefore it can be concluded that the effect of reinforcement by an extensible material, such as non-woven fabric, appears after the settlement of an embankment exceeds 4% of the height of the embankment.

According to the observation of model after loading tests in the case of Test No 3, the first and second non-woven fabric from the top of embankment were torn at two lines and the third one was torn at one line and the fourth one was not damaged.

Fig. 3 shows the relationship between the load and the settlement of the top of an embankment with a vertical slope when a

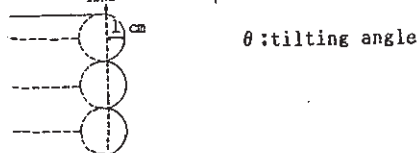
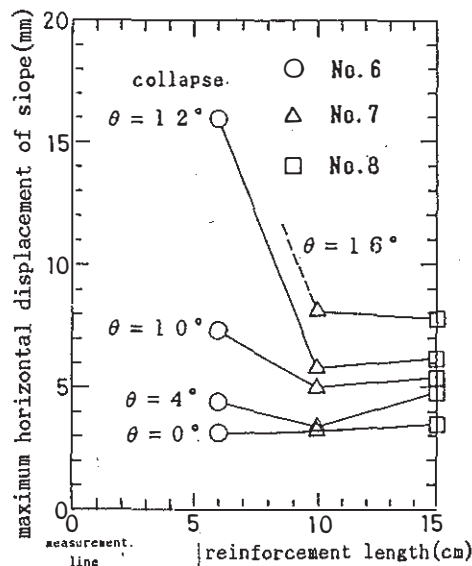


Fig. 4 Maximum horizontal displacement of slope and placement length of non-woven fabric

vertical load was applied to the model embankment with a hydraulic piston. This figure indicates that the peak vertical load and the settlement of the top of an embankment at peak increase with the increase of fabric reinforcement length L.

For example the peak vertical load of Test No. 11 (L = 24.2cm) was about 3.5 times larger than that of Test No. 9 (L = 6cm).

Therefore the reinforcing effects of increasing the reinforcement length of fabric are clearly observed in the figure.

Fig. 4 denotes the relationship between the maximum horizontal displacement of a slope and the reinforcement length of non-woven fabric. The maximum displacement of the slope was measured using photographs.

The maximum displacement of slope in Test No. 6 with the reinforcement length of 6cm was about 40% larger than that of Test No. 7 and No. 8, with the reinforcement length of 10cm and 15 cm, respectively, when the tilting angle was 10 degrees. It was almost the same in Tests No. 6, No. 7 and No. 8 if the tilting angle was less than 4 degrees. The embankment in Test No. 6 collapsed when the tilting angle increased to 12 degrees, but it did not collapse in Tests No. 7 and No. 8 even if the tilting angle was 16 degrees.

These test results indicate that the reinforcement length of fabric considerably affects the stability of reinforced embankment subjected to horizontal force.

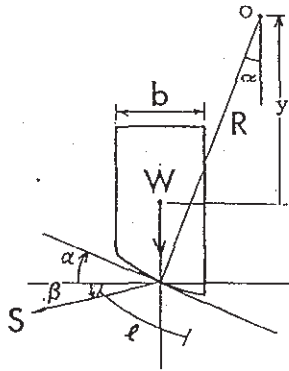


Fig. 5 Slice for stability analysis

## 6 STABILITY ANALYSES

Stability analyses were performed assuming a circular slip surface. The safety factor for stability of a slope with reinforcing fabric is expressed by the following equation.

$$F_s = \frac{ER[c + ((W - ub)\cos\alpha - k_h W \sin\alpha + S \sin(\alpha + \beta)) \cdot \tan\phi]}{\sum [RW \sin\alpha + yk_h W - RS \sin(\alpha + \beta)]} \quad (3)$$

where R: radius of slip circle, c: cohesion, l: length of circular arc of a slice, W: weight of a slice, u: pore water pressure, b: width of a slice,  $\alpha$ : angle between a vertical line and a line which connects the center of the slip circle to the center of the circular arc of a slice (see Fig. 5),  $\beta$ : angle between a horizontal line and reinforcing material (see Fig. 5), S: tension which acts in reinforcing material,  $\phi$ : angle of internal friction,  $k_h$ : horizontal seismic coefficient.

The tension S which acts in the reinforcing fabric is taken as the smaller of the pull-out strength  $S_1$  which is determined from Eq. (4) and the tensile strength  $S_2$ .

$$S_1 = 2 \times \mu \times \sigma'v \times B \times L' \quad (4)$$

where  $\mu$ : friction coefficient between soil and reinforcing fabric,  $\sigma'v$ : effective overburden pressure, B: width (= 1m), L': reinforcement length from the intersection of slip surface and reinforcing fabric.

The friction coefficient  $\mu$  was 1.0 for the fabric and the sand used in this series of tests, which was determined from a pull-out test of fabric in sand. It was assumed that the angle of internal friction  $\phi = 0$  for the half of sandbags opposite to the backfill. For Tests No. 6, No. 7, and No. 8 the minimum safety factor of stability was calculated by changing slip surface, because it was quite difficult to determine a particular slip surface from the distribution of principal strains for Tests No. 7 and No. 8.

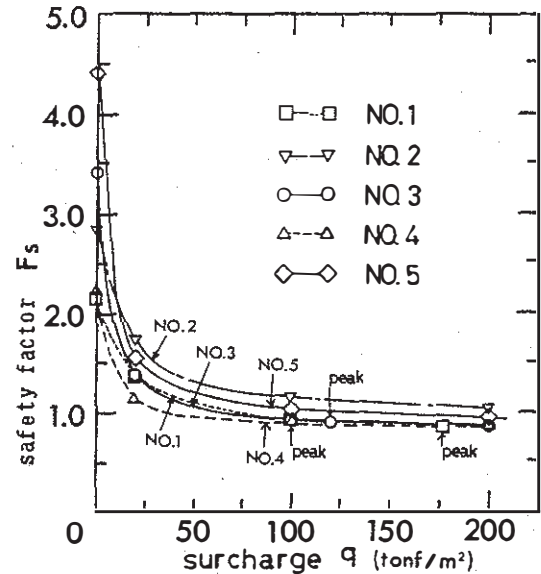


Fig. 6 Safety factor and surcharge (Test No 1 ~ No5)

For other tests, the safety factor of stability was calculated assuming a circular slip surface for each model from the distribution of principal strain.

In the tests, a slip surface was compulsively developed by vertical loading, and therefore the safety factor was calculated against a slip circle which was most similar to the observed slip surface. The results of calculation are shown in Fig. 6. In the calculation the maximum tensile strength at peak of non-woven fabric was substituted for S in Eq. (3). The arrows in Fig. 6 show the point where the load reached a peak value, and the corresponding safety factor was about 0.9 for Tests No. 1, No. 3, and No. 4. It can be estimated that the sliding soil mass began to create a large slide when the load reached a peak value. Fig. 6 shows that the safety factor calculated by Eq. (3) for such a condition was about 0.9, therefore the evaluation of stability by Eq. (3) gives reasonable results. The comparison among the results of Tests No. 3, No. 4 and No. 5 in Fig. 6 indicates that the safety factor increases with an increase in the number of non-woven fabrics placed in an embankment.

Fig. 7 shows the relationship of the minimum safety factor vs. the model tilt angle  $\theta$ . This figure indicates that the minimum safety factor for Test No. 6 becomes almost 1.0 when the tilting angle  $\theta$  is 10 degrees and becomes smaller than 1.0 when  $\theta$  is 12 degrees. This calculation provides a reasonable explanation of why Test No. 6 collapsed when the tilting angle was 12 degrees during the test. The safety factor for Test No. 7 and Test No. 8 is larger than 1.0

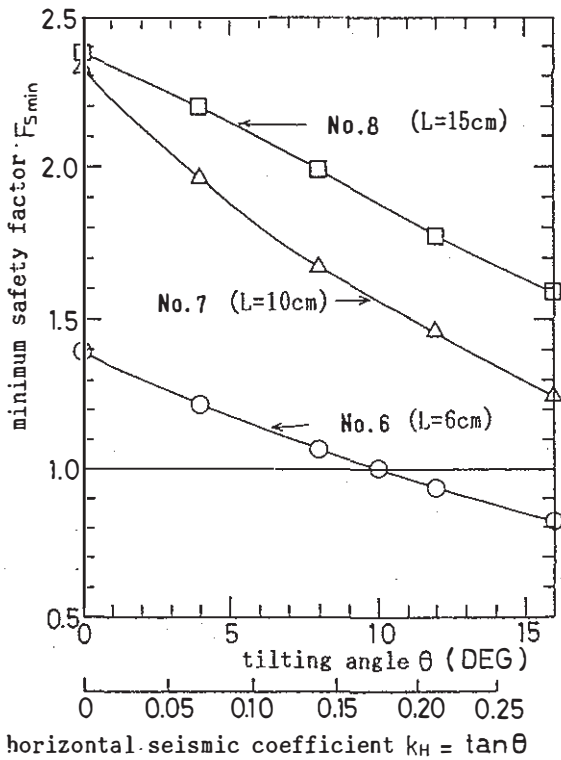


Fig. 7 Minimum safety factor vs. tilting angle (Test No 6 ~ No8)

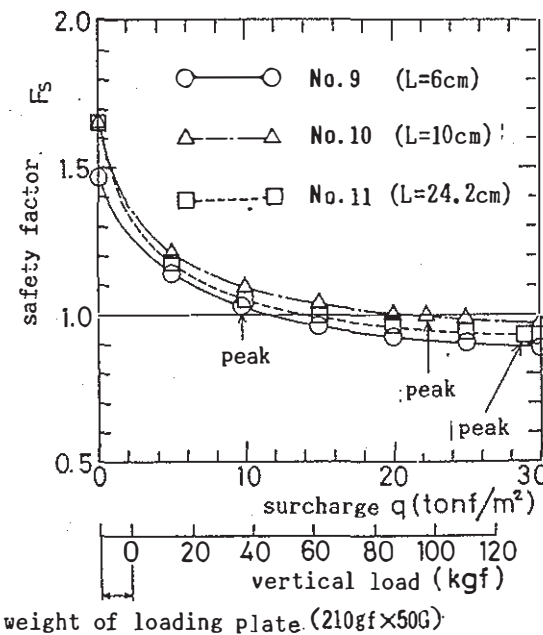


Fig. 8 safety factor vs. surcharge (Test No 9 ~ No10)

for the tilting angle  $\theta = 0 - 16$  degrees, which well agree with the test results that Tests No. 7 and No. 8 did not collapse when the tilting angle became 16 degrees. It can be noted from Fig. 7 that the minimum safety factor is larger for models with longer fabric reinforcement lengths.

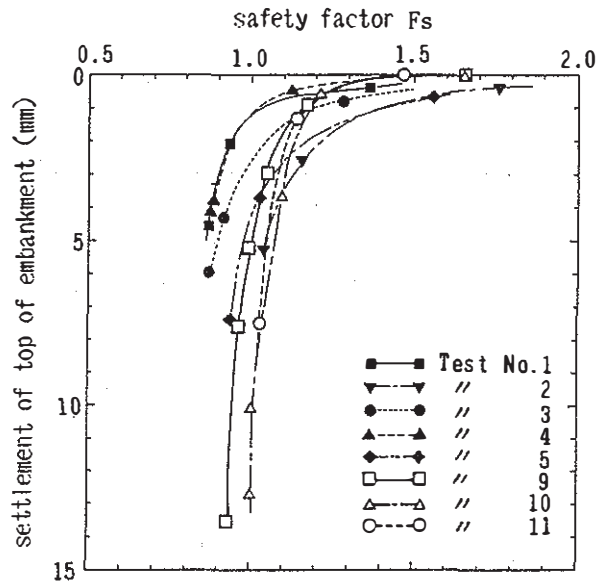


Fig. 9 safety factor vs. settlement of embankment

Fig. 8 shows the relationship between the safety factor for the observed slip surface and the surcharge for Tests No. 9, No. 10, and No. 11. In this figure the safety factor is in the range of 0.95 - 1.05 when the applied vertical load is at peak. The change of safety factor due to the change of reinforcement length of fabric is as small as about 0.1.

Fig. 9 shows the relationship between the safety factor and the settlement of the top of the embankment, shown in Fig. 2 and Fig. 3, for the eight cases in which vertical loads were applied to the top of the embankment. In this figure most data show that the settlement of the top of the embankment is very small if the safety factor is more than about 1.0, but the settlement increases extremely if the safety factor becomes less than about 1.0. Similar tendency appeared also in shaking table tests conducted by one of the authors et al. (Koga et al. 1988)

#### 7 A COMMENT ON STABILITY ANALYSES

Eq. (3) to calculate a safety factor of a reinforced embankment was derived by extending the Fellenius method to incorporate the effect of tension of non-woven fabric to intersect a slip surface. The tension  $S$  has different meaning in a strict sense in the numerator and denominator in the equation. While the former, resistant moment, should reflect the value at the failure occurrence, the latter, driving moment, should be that to balance the slice.

The same value of tension was used in the above stability analyses for their simplicity. However, it must be noticed that this

equation becomes irrational if the tension  $S$  is great, because the denominator becomes negative.

Further study is needed to select the most appropriate equation for stability analysis of reinforced embankment.

In the proper equation, it is desired that a safety factor of embankment against sliding should have the following continuity under several conditions.

- ① The safety factor without reinforcement is not so different from that with little reinforcement.
- ② The safety factor under no seismic force is not so different from that under a small seismic force.

## 8 CONCLUSIONS

(1) The reinforcement by fabric can be strengthened by increasing the reinforcement length, or the number of sheets of fabric in both cases of an inclined slope and a vertical slope. In the case of tilting tests, the horizontal displacement of the slope of reinforced embankment became smaller for the longer fabric reinforcement length.

In the case of applying vertical loads to the top of an embankment, both the peak value of load and the settlement of the top of the embankment when the load was at peak increased with the increase of the reinforcement length or the number of sheets of fabric.

(2) An nearly circular arc slip surface was observed when a fabric reinforced embankment collapsed or had large deformation due to tilting or applying vertical loads. Calculations on the slope stability assuming a circular slip surface well agreed with the centrifugal test results.

## ACKNOWLEDGEMENTS

The authors would like to express their appreciation to Mr. S. Washida of P.W.R.I. for his help during the model tests and analyses.

## REFERENCES

- 1) Tatsuoka, F. et al. (1985); Reinforcing of Cohesive-Soil-Embankment with Un-Woven Fabric (in Japanese), *Tsuchi-To-Kiso*, Vol.33, No.5, pp.15-20.
- 2) Taniguchi, E. et al. (1986); Centrifugal Model Tests on Geotextile Reinforced Embankments, Proc. of 8th Asian Regional Conf., ISSMFE, Kyoto, Vol.1, pp.499-502.
- 3) Taniguchi, E., Koga, Y., Morimoto, I. and Yasuda, S. (1988); Centrifugal Model

Tests on Reinforced Embankments by Non-Woven Fabric, Proc. of the Int. Conf. on Geotechnical Centrifuge Modelling, Paris, pp.253-258.

- 4) Koga, Y., Ito, Y., Washida, S. and Shimazu, T. (1988); Seismic Resistance of Reinforced Embankment by Model Shaking Table Tests, Int. Geotechnical Symposium on Theory and Practice of Earth Reinforcement, Fukuoka, submitting.